



Anti-bacterial and Anti-biofilm Effect of Curcumin-Ag Nanoparticles against *Pseudomonas aeruginosa* Isolated from Iraqi Burn Patients Infections

Rasha Mohammed Sajet Al-Oqaili^{*1,2}, Seyyed Meysam Abtahi Froushani¹,
and Likaa Hamied Mahdi²

¹Department of Microbiology, Faculty of Veterinary Medicine, Urmia University, Iran

²Department of Biology, College of Science, Mustansiriyah University, Iraq

Abstract: The increasing emergence of multidrug-resistant bacteria, which are the cause of wound infections, constitutes a major health problem, and because of their ability to produce biofilms. The main objective of the present study is to evaluate the antibacterial and antibiofilm activity of curcumin-Ag nanoparticles. According to Scanning Electron Microscopy (SEM) and X-Ray Diffraction analysis (XRD), the nanoparticles appeared in spherical shapes and sizes of 47.98 - 58.80 nm. From UV-Visible spectrum a high-intensity absorption peak around 450 nm called the spectral plasmonic region (SPR), is observed for curcumin-Ag. To examine the antibacterial activity, the agar-well diffusion method was performed. Minimum inhibitory concentrations (MIC) of curcumin-Ag nanoparticles and gentamicin were used to evaluate the antibacterial activity against resistant *Pseudomonas aeruginosa*. The results indicate that nano-curcumin possesses material anti-bacterial activity against all *Ps. aeruginosa* isolates disparity with control, and the anti-bacterial activity of nano-curcumin at 256 µg/ml was significantly higher than 128 µg/ml, according to earlier research, curcumin nanoparticles break down bacterial cell walls, and when this happens, the bacteria lyse and die. Antibiotic susceptibility testing was performed on Piperacillin (70%), Imipenem (53.33%), Colstine (40%), Gentamycin (0%), and Ceftaroline (CFT) (30%). Significant antibacterial action of curcumin NPs was observed against the most biofilm-producing *Ps. aeruginosa* isolates.

Keywords: Antimicrobial Activity, Antibiofilm, Burn, Curcumin Silver Nanoparticles, Characterization, *Pseudomonas aeruginosa*.

1. INTRODUCTION

Burn patients are more susceptible to hospital-associated infections, when the skin is burned, it disrupts the physiological function of the immune system and destroys the skin's protection from infection [1]. *Ps. aeruginosa* is a Gram stain-negative (-) bacillus. It is aerobic and causes unscrupulous or nosocomial contagion in burn patients, wound infections, cystic fibrosis, and folks who suffer from immunodeficiency [2]. Furthermore, the development of biofilms, which are of a vital and critical virulence factor that improves the survivability of bacteria in these settings, what allows bacteria to survive in harsh environments, such as drought or the presence of

disinfectants [3]. Formation of biofilms is one of the reasons aimed at antibiotic resistance, and also serve as a partition between antibiotics and bacterial cells or immune responses [4]. Furthermore, in the case of burn injuries, eschar formation prevents access of host immune cells to the infected area and systemic administration of antibiotics [5]. Most are susceptible to anti-pseudomonal antibiotics, but the difficulty of eradication adds to the problem of burn management. Burn injuries are chronic and incurable diseases that are difficult to treat due to the evolution and changes in the antimicrobial properties of the pathogens involved. Curcumin is a major phytochemical resulting from *C. longa* (Zingiberaceae), which is known as turmeric, a naturally occurring yellow

Received: April 2024; Revised: February 2025; Accepted: March 2025

* Corresponding Author: Rasha Mohammed Sajet Al-Oqaili <stry@uomustansiriyah.edu.iq>

pigment [6]. When combined with other drugs, this compound has anticancer and antioxidant properties [7, 8]. Extensive research conducted over the past 50 years indicates that curcumin has powerful antioxidant, anti-inflammatory, anti-tumor, anti-HIV, and antimicrobial effects [9-12]. Nanoparticles have singular properties in electronic, magnetic, and chemical energizing. Nanoparticles are also characterized via loudly stability, lack of reaction, biocompatibility, and comparatively shortage of toxicity. That is why these are widely applied in numerous domains of biomedicine, such as industry, gene delivery, etc. Certain mineral nanoparticles also have antiviral, antibacterial, antifungal, and antitumor possessions [13]. In general, there are three requisite methods for building nanoparticles: Chemical methods, Physical methods and Biological methods [14].

Silver nanoparticles (Ag-Nps) are the most studied and most widely used of all nanoparticles. Ag-Nps are now regarded as next-generation antibiotics. This is because these are highly effective in suppressing microorganisms. Ag-Nps are currently the leading nanoparticles among all commercialized nanomaterials. Research into their use as antibacterial agents has intensified over the years due to their low toxicity compared to other nanoparticles. Adherence and penetration of Ag-Nps onto microbial membrane surfaces is typically the first step in their cytotoxic mechanism [15]. One of the drawbacks of the synthesis of chemical and physical methods is that these are comparatively expensive, adding to chemical methods involving the use of elements and compounds. It has poisonous and risky effects on researchers, and some hazards are graver than the environment or neighborhood in which it is located. Lives in it because several physical and chemical mechanisms lead to the generation of nanoparticles that are not suitable. You can't control the shape, size, and purity you need, so you have to find a way safer, more accurate and cheaper [16]. Alternatively, a method known as the green method produces a more homogenous material Fewer defects resulting from nanoparticle formation by microorganisms such as bacteria and fungi or algae, plants, or plant extracts, many characteristics of organisms such as pathways Biochemical, enzymatic activity, stage of cell growth, and optimal response are considered Defines a selection of objects or their extracts for building nanoparticles [17]. Researchers have

looked into the special qualities of synthesized green nanoparticles [18]. As a result, nanoparticles are increasingly being used in medicine development, coatings, and food packaging [19, 20]. It has been demonstrated that using nanoparticles as carriers in drug delivery systems increases bioavailability, stability, pharmacological, and solubility effect while preventing cytotoxicity to healthy cells, chemical and physical dissolution, and excessive dose requirements. Because of their numerous potential applications as antibacterial, antifungal, antioxidant, anticancer, and anti-inflammatory medicines, silver nanoparticles (Ag-Nps) have piqued the interest of researchers and scientists [21]. Ag-Nps can withstand a broad variety of temperatures and are far less volatile than other nanoparticles [22], that can limit microbial development after initially coming into contact with bacteria [23]. For the management of *Ps. aeruginosa* infections in those who already have them, new medications and other therapies must be created right away when traditional antibiotics become ineffective. New antibiotics with distinct modes of action, novel dosage techniques, and resistance to bacterial enzyme changes have all been the subject of recent research [24, 25]. The aim of this research is to explore for substitutes, such as nanomaterials, which have emerged as a promising alternative to antibiotics in recent years, such as the antibacterial and antibiofilm activity of curcumin-Ag nanoparticles. We hope that the present research findings will address the growing problem of multidrug-resistant bacteria, which cause wound infections and are a major health concern due to their capacity to form biofilms.

2. MATERIALS AND METHODS

2.1. Synthesis of Curcumin Silver Nanoparticles

To get a final concentration of 10.6 μ M, a tiny amount of an ethanolic solution of curcumin (10.6 mM, 1 ml) was first dispersed in 1 L of ultrapure water. The pH of the solution was brought to 8.5 - 9 by a tiny amount of 1 M NaOH. A little amount of AgNO₃ (1 mM, 1 ml) solution was added to 99 ml of boiling curcumin solution at a moderate stirring speed (350 rpm) in order to produce particles. For 48 hours, the resultant solution was dialyzed against 10 mM borax buffer, with a dialysis medium change occurring every 24 hours [26]. After making certain adjustments to the green color

compositing procedure, we carefully examined the results using the Bettini protocol to obtain the naturally occurring silver-capped NPs compound, also known as curcumin-Ag [26]. The purpose of the synthesis was to address the issue of lengthy contact times. We used a reaction flask, instead of an oven with adequate ventilation, to conduct the Curcumin-NP reaction. The Bettini method called for carefully adjusting the pH and raising the reaction temperature from 90 to 100 °C [27].

2.2. Characterization of Curcuma Silver Nanoparticles (Cur-Ag-Nps)

X-ray diffraction (XRD) is being used to characterize the phase identification, structure of crystals, composition and physical characteristics of curcumin nanoparticles. The nanomaterial is deposited on a piece of glass to measure it by (a Lab XRD Shimadzu XRD-6000) in Iran. A high-precision vertical goniometer built-in X-ray diffraction is dependent on monochromatic X-ray constructive interference and a crystalline sample. The KBr technique was used to obtain the Fourier transform infrared spectrum (FTIR). The material is pressed into a disc after being combined with KBr in a (1:1) molar ratio. A little quantity of moisture was put on a glass slide to dry before measurement, and measurements were run in the wavenumber range of 600 to 4000 cm^{-1} to evaluate and determine the functional groups present in the produced curcumin nanoparticles. It should be stored in a dust-free environment overnight before being measured. Field Emission Scanning Electron Microscopic (FESEM) study was conducted using VEGA 3 (TESCAN, Czech Republic) SEM machine. SEM was used to visualize the morphology and nanoparticle grain size of tested samples. Thin films of curcumin nanoparticles were prepared on the cover slide grid by reducing the amount of solution on the cover slide and then allowed to dry at room temperature before being visualized under SEM. The hydrodynamic diameter of the curcuma silver nanoparticles (Cur-Ag-Nps) and their possibility were gauge through the Dynamic light scattering (DLS) technique, whereas the TEM pictures obtained with a JEOL 1200 EX TEM running at a 120 KV acceleration voltage were statistically analyzed to determine the diameter of the particles' silver center. UV-analysis using Spectral ax was used to determine the existence and make-up of the curcuma shell encircling the particles [28]. These

characterizations were carried out at the College of Science, Mustansiriyah University, Iraq.

2.3. Sources of Clinical Bacteria Isolates

Thirty (30) bacterial isolates belonging to *Pseudomonas aeruginosa* were isolated from people with burns and lying in bed in Yarmouk Hospital in the city of Baghdad. The diagnosis of the bacteria as *Pseudomonas aeruginosa* was confirmed using the Vitek 2 device.

2.4. Testing of Antibiotic Susceptibility

Testing susceptibility of antibiotic was executed by the Kirby power disk diffusion method; this method is described in details elsewhere [29]. Antibiotic tablets Cefaroline (CFT) (30), Colstine (CT) (10), Gentamycin (GN) (10), Imipenem (IMP) (10), and Piperacillin (PRL) (10) were used for antibiotic susceptibility testing (AST). According to Magiorakos *et al.* [30], isolates that show resistance to three or more distinct types of antipseudomonal drugs are classified as multidrug resistant (MDR). In this study, *Escherichia coli* ATCC strain 25922 was used for quality control.

2.5. Biofilm Formation Assay

Two diverse methods, Congo red agar (CRA) and microtiter plate assay (MPA), were used to detect biofilms in each isolate. Biofilm production by all isolates was detected using the CRA method, as reported previously [31, 32]. All isolates were grown on Congo red agar (CRA) and examined for biofilm production. For the MPA method, as stated by Zhang *et al.* [33], the identified and purified *Pseudomonas aeruginosa* bacterial isolates were transferred to Vortex to mix and homogenize them well, then they were placed in a liquid medium (Luria-Bertani broth) for the purpose of culturing them for 18 hours at 37 °C. 96-well microtiter plates were used, and the bacterial isolates were transferred to these plates. Then the microtiter plates were transferred to the incubator at a temperature of 37 °C for 18 hours. A spectrophotometer was used at a wavelength of 540 nm. The range of the optical density was 0.56 to 0.64. Following the incubation time, 96-well microtiter plates were filled with 25 ml of 1% crystal violet per well. After letting them sit at room temperature for fifteen (15) minutes, thoroughly wash each with 200 milliliters of sterile

buffer, PBS. A UV spectrophotometer (Shimadzu, Japan) was used to detect the absorbance at 540 nm after crystal violet was dissolved in glacial acetic acid to gauge the degree of biofilm formation. Using crystal violet as a control to wells that are exposed to a medium devoid of germs, every assay was run in triplicate [34].

2.6. Determination of Nano-Curcumin-Ag and Gentamicin MIC and Sub MIC

Depending on the micro dilution method described by Elshik *et al.* [35] different concentrations of gentamicin and Nano-curcumin-Ag (1-1024 µg/ml) melted in Muller-Hinton broth (MHB) were prepared from a stock solution in a 96-well polystyrene microtiter plate. The bacterial *P. aeruginosa* suspension (10 µl) adjusted to 0.5 McFarland standard was additional to each well except for the monitoring of negative wells contained gentamicin culture was considered as a positive well, the microtiter plate was incubated overnight at 37 °C. Resazurin (0.015%) was additional to all wells (30 µl per well) and incubated for an additional 2-4 h to observe any color change after 24 h at 37 °C, after the incubation period was through columns with no color change the blue resazurin color stayed the same after the incubation period was through, columns with no color change (the blue resazurin color stayed the same) given a score the MIC value.

2.7. Antibiofilm Activity of Nano-Curcumin-Ag and Gentamicin Sub-MIC Against *Ps. aeruginosa* Isolates

Biofilm development was investigated using the same procedure as described previously [36]. Each well received 180 µl of nano-curcumin-treated BHIB and sub-MIC gentamicin, 20 µl of *Ps. aeruginosa* suspension, and a control of 0.5 MacFarland after sterile tryptic soy broth with 2% sucrose was prepared. Following incubation, the medium was taken out of the wells, rinsed three times with sterile buffer (PBS) to get rid of any remaining *Ps. aeruginosa* cells, and allowed to dry for fifteen (15) minutes at room temperature. After adding 200 µl of 0.1% purple crystals, waited for 20 minutes. The stained wells were rinsed three times with PBS (PH 7.2) and allowed to dry at room temperature for 15 minutes in order to eliminate any remaining dye. The optical density was then measured after 200 µl of 95% ethanol was added to

each well, by using ELISA reader at 630 nm.

2.8. Antibacterial Activity of Nano-Curcumi-Ag Against *Ps. aeruginosa* Isolates

Used the agar well diffusion method to detection antibacterial activity of nano-curcumin against *Ps. aeruginosa* at concentrations of 128 µg/ml and 256 µg/ml, according to the procedure described by Kunwa *et al.* [37].

2.9. Statistical Analysis

The obtained data were subjected by analysis of variance (ANOVA) test to compare the means of various groups with each other. LSD test was used to calculate the significant differences between tested mean, the letters (A, B, C, and D) LSD for rows represented the levels of significant, highly significant start from the letter (A) and decreasing with the last one. Similar letters mean there are no significant differences between tested mean. Results were expressed as mean ± SD and values of $p > 0.05$ were considered statically non-significant, while $p < 0.05$, < 0.01 , and 0.001 were considered significantly different, highly significantly different respectively. The statistical analysis was carried out by SPSS (v 20).

3. RESULTS AND DISCUSSION

3.1. Synthesis of Curcumin Silver Nanoparticles

Color change of the resulting colloidal material is shown in Figure 1; this solution confirmed the formation of Cur-Ag-Nps, which was subsequently confirmed by UV-visible spectroscopy. The results were similar to a previous study by Khan *et al.* [18].

3.2. Characterization

Following synthesis, it was eliminated by

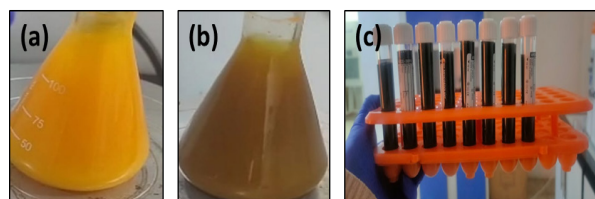


Fig. 1. Synthesis of Curcumin Silver Nanoparticles, (a) Curcumin solution, (b) Curcumin & AgNO₃, and (c) Cur-Ag-Nps.

hemodialysis, where ultrapure water for borax buffers was used for NP, after the pH was decreased and the reaction residue was removed. To make Bettini's synthesis mixes as biocompatible as possible without sacrificing particle stability, we used a buffer (borax). The buffer was concentrated to a level that eliminated the possibility of osmotic stress-induced, which can harm to human cells during exposure. According to the nanoparticles' X-ray diffraction study results (Figure 2). The diffraction peaks at angles (2θ) of 38.2359° , 44.3076° , 64.5258° , and 77.4274° can be attributed to crystalline lattices (111), (200), (220), and (311), respectively of the face-centered cubic crystalline structure that accorded with the standard silver card values (JCPDS No.87-0720). Its purity and highly crystalline quality are indicated by the highest peak, which is found at 38.2359° . The XRD profiles of curcumin-loaded Ag-Nps, as shown in Figure 2, affirming its highly crystalline nature [38]. The XRD pattern of curcumin-loaded Ag-Nps

also displayed characteristic peaks within the 2θ confirming the successful conjugation of curcumin onto the synthesized nanoparticles [39].

The ground sample's SEM revealed that the particles were synthetic, with an average diameter of 47.98 - 58.80 nm (Figure 3). The dried curcumin nanopowder was discovered to have good chemical and physical stability. Similar findings from earlier studies have indicated that reducing the active component's particle size to nanoparticle size improves its solubility and bioavailability [13]. It should be noted that these results agree with the previous XRD data [38, 39], that were obtained using the same preparation process. Gevorgyan *et al.* [40] also prepared nanoparticles using various techniques for cardiovascular complications.

FTIR is a powerful technique that works on the principle that ligand clusters vibrate at different frequencies. It can be used to detect functional

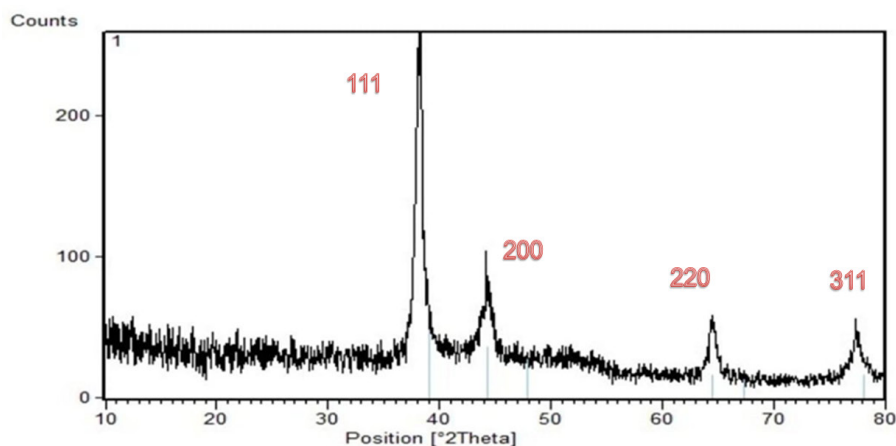


Fig. 2. Powder X-ray diffraction (XRD) of curcumin NPs.

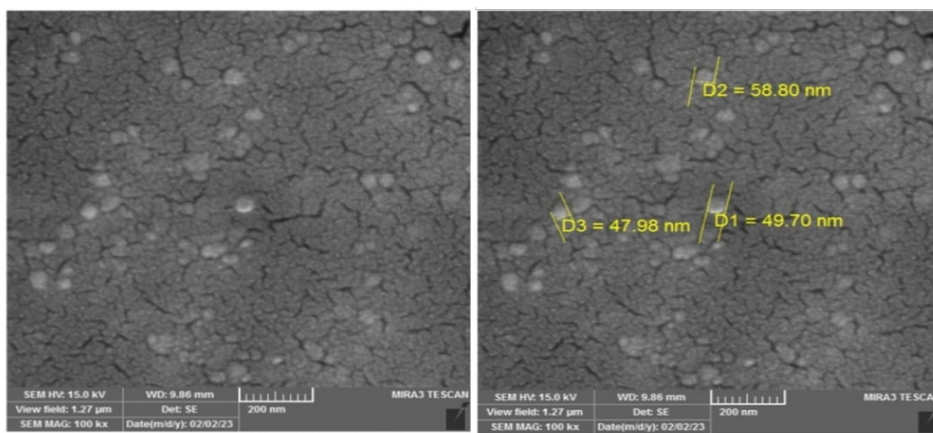


Fig. 3. Scanning Electron Microscopy SEM Analysis of Curcumin nano particles.

groups and characterize covalent bonds. FTIR spectrum of nano-curcumin is shown in Figure 4, where peaks are observed at 2594.04, 1842.22, 1264.04, and 927.61 cm^{-1} . The broad stretch at 3435.91 cm^{-1} represents the stretching vibration of the frequency (stretching) of the O-H bond with the hydrogen bond present in curcumin nanoparticles. The sharp peak at 2594.04 cm^{-1} indicates O-H stretching bonds of the functional group, carboxylic acid. The sharp peak at 2076.41 cm^{-1} indicates CH stretching of methylene groups. The sharp peak at 1842.22 cm^{-1} indicates C=O stretch bonds of functional group anhydride. The sharp peak at 1633.84 cm^{-1} is the stretching vibration of C=O and C=C double bonds. The sharp peaks at 1264.04 cm^{-1} and 1025.98 cm^{-1} C-N bonds of functional group amines. The sharp peak at 927.61 cm^{-1} C-O bonds of functional group anhydrides. The sharp peak at 703.57 cm^{-1} represents the C-Cl bonds of functional group alkylhalides. These results are consistent with the research of Joly and Latha [41], who showed that nanocurcumin has strong intensity and sharp peaks.

Figure 5 shows the UV-Visible spectrum of curcumin silver nanoparticles (curcumin-Ag-Nps) in high-purity water. A high-intensity absorption peak around 450 nm called the spectral plasmonic region (SPR), is observed for curcumin NPs. These results are consistent with the previous studies [28, 41]. The UV-visible spectroscopy can be used to verify nanoparticle constancy, or the stability of nanoparticles in liquid. When the particles lose their stability, or become destabilized (due to the exhaustion of stable nanoparticles), the intensity of the initial extinction value decreases.

Several images were taken using delivery transmission electron microscopy (TEM) in order to examine the size of Cur-Ag-Nps and calculate their average silver core diameter (Figure 6 (a, b)). After that, the images were processed using image analysis software (ImageJ) to determine the diameter of each particle in each picture. The TEM images of curcumin-Ag nanoparticles reveal that the nanoparticles are spherical in shape, and the average size is about 50 nm.

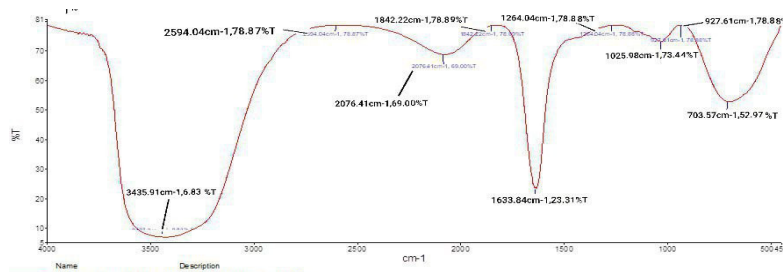


Fig. 4. Fourier transform infrared (FTIR) for identification of encase compounds in curcumin-Ag-NPs.

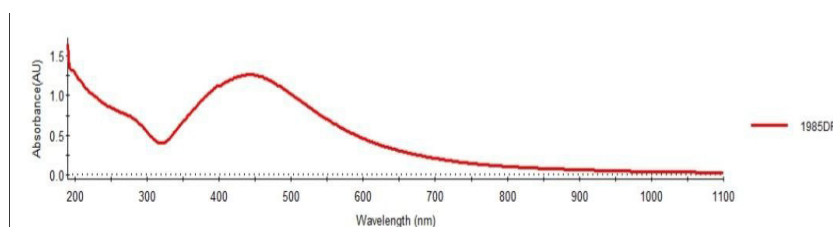


Fig. 5. UV-Visible spectrum of Curcumin NPs.

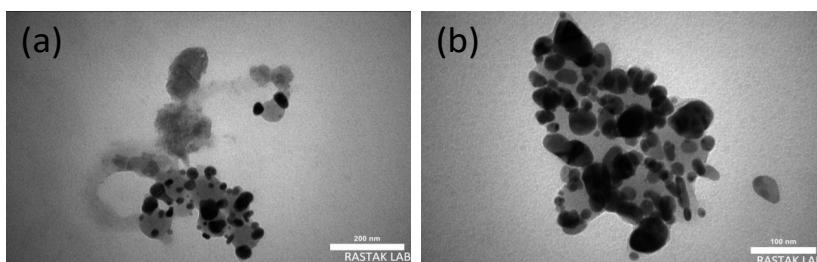


Fig. 6. Transmission electron microscopy (TEM) images of Cur-Ag-Nps. (a) 7500x magnification and (b) 10,000x magnification.

Figure 7 shows the DLS investigation of Cur-Ag-Nps dispersions using dynamic light scattering. The curcumin shell and the amount of water bonded to it have a direct impact on the electrostatic charge since DLS assesses the molecule's hydrodynamic diameter [43]. Large particles scatter more light than small particles, hence DLS tends to overestimate them [44]. The material's electron density in relation to the supporting carbon lattice determines how different the TEM image is. Because of this, the molecule's curcumin layer is thin and nearly impossible to photograph using TEM imaging because of its poor contrast [45]. Similar findings were found in earlier research, which demonstrated that the active element's efficacy, solubility, and bioavailability are increased when its particle size is reduced to nanoparticle size [46].

3.3. Antibiotic Susceptibility Test for *P. aeruginosa* Isolates

The antibiotic susceptibility test (AST) was managed for the isolates of bacteria *Ps. aeruginosa* using the disc diffusion process with five antibiotics

from dissimilar classes. The results of antibiotic susceptibility of *Ps. aeruginosa* showed that 70% of isolates were resistant to Piperacillin follow by 53.33% resistant to Imipenem (FEP), 40% were resistant to Colistine, 30% were resistant to Ceftaroline, and 0% *Ps. aeruginosa* isolates were resistant to Gentamycin, these results are shown in Figure 8. It is unclear from the results if gentamicin is the most effective medication when compared to other antibiotics; this could be because the isolates have various antibiotic resistance mechanisms. Various antibiotics, particularly those in the minoglycoside class, cause *Pseudomonas aeruginosa* to develop resistance to pharmacological classes known as beta-lactams and quinolones [47]. Another study by Akingbade *et al.* [48] showed that *Pseudomonas aeruginosa* contains a large number of resistance genes, including extended resistance genes. A spectrum of β -lactamases (ESBLs), aminoglycoside-modifying enzymes (AMEs), and β -lactamases shows that they can rapidly mutate and acquire drug resistance to adapt to the environment and spread resistant bacteria [49]. The incidence of antibiotics is increasing year by year [50].

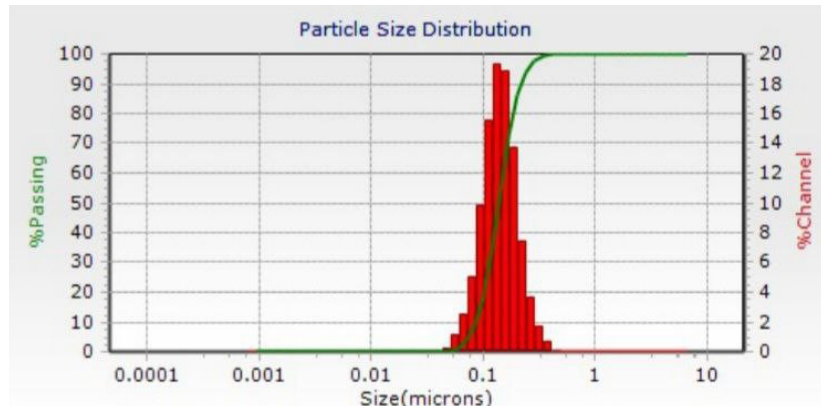


Fig. 7. Dynamic light scattering DLS analysis of “curcumin silver nanoparticles” “Cur-Ag-NPs” dispersions.

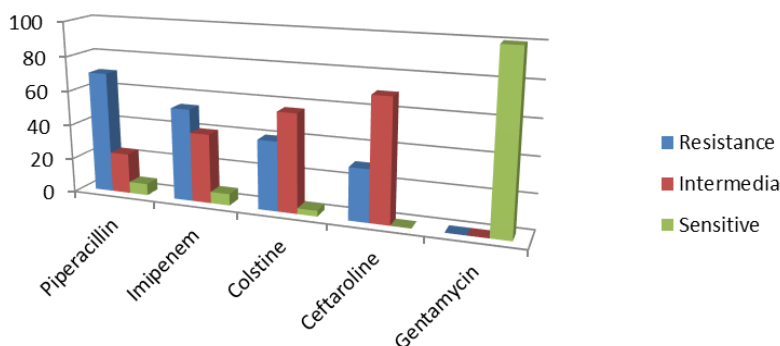


Fig. 8. Results of antibiotics susceptibility test to *Pseudomonas aeruginosa*.

3.4. Biofilm Formation of *Ps. aeruginosa*

Ps. aeruginosa have probable biofilm formation capability on Congo Red Agar (CRA). The colony color of isolates changes to black, an indication of the productivity of biofilms (Figure 9), and biofilm formation capability on the microtiter plate (Figure 10). The obtained results were labeled into 4 groups (non-biofilm production, weak, moderate, and strong) based on threshold values. Based on the criteria listed in Table 1 of the 30 *Ps. aeruginosa* isolates in this study, 3 strains formed weak biofilms, 11 strains formed moderate biofilms, and 16 strains were shown to have formed a strong biofilm. Cutoff values for *Ps. aeruginosa* isolates are summarized in Table 1. The result showed only 53.3% of *P. aeruginosa* isolates were strong producers for biofilm, while 36.7% and 10% of the isolates were moderate and weak producers for biofilm, respectively. This was mentioned in a previous study of 100% of *Ps. aeruginosa* isolates are biofilm productive [51], which supports our



Fig. 9. Biofilm formation by *Ps. aeruginosa* on Congo Red Agar, it contains (brain heart infusion broth, sucrose, agar and Congo red solution).

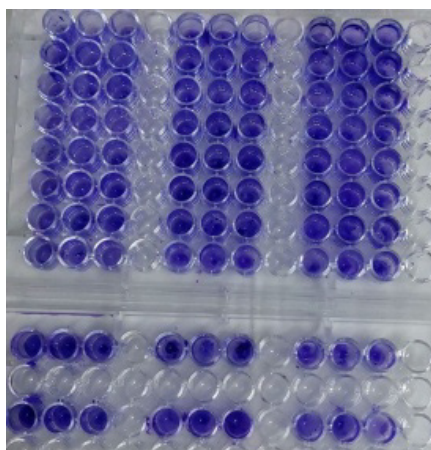


Fig. 10. Biofilm formation by *Ps. aeruginosa* on microtiter plate.

findings. Numerous studies have demonstrated that *Pseudomonas aeruginosa* MDR produces more biofilms than other harmful bacteria, demonstrating the synergistic influence of biofilm formation and antibiotic resistance.

3.5. Determination of Nano-Curcumin-Ag and Gentamicin MIC and Sub MIC

The four isolates of *Ps. aeruginosa* that produced the most biofilm (No. 12, No. 14, No. 25, and No. 26) were examined for their susceptibility to gentamicin and nano-curcumin. It was observed that isolates varied in their susceptibility to gentamicin and nano-curcumin. Gentamicin was employed as a control since clinical isolates were responsive to it (Table 2).

3.6. The Antibiofilm Activity of Nano-Curcumin and Gentamicin Sub MIC Against *Ps. aeruginosa* Isolates

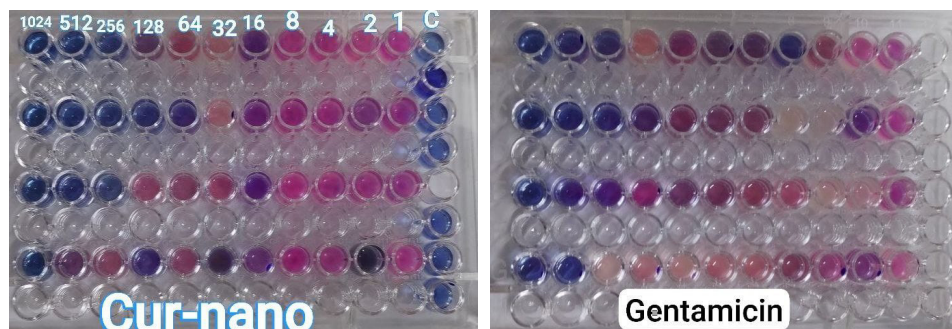
Nano-curcumin shows a significant antibacterial film activity against the tested isolates of *Ps. aeruginosa* no. 6 biofilm ($OD\ 1.732 \pm 0.236$, reduced to 0.216 ± 0.065) and no. 12 biofilm ($OD\ 0.987 \pm 0.152$, reduced to 0.194 ± 0.145). In contrast, the OD of the no. 15 biofilm decreased to 0.309 ± 0.109 from 1.589 ± 0.178 . In vitro, nano-curcumin exhibited more anti-biofilm action than gentamicin, as illustrated in Figure 11. Using treatments with minimum inhibitory concentrations (MIC values), such as gentamicin and nano-curcumin, is one way to eliminate biofilms formed by previous isolates [51]. It has been reported that the minimum inhibitory concentrations (MIC) of gentamicin and amikacin are utilized to reduce the growth of biofilms on plastic sheets. Several studies have shown that some pure substances, like bacteriocins and enzymes, have potent anti-microbial and anti-biofilm qualities that outperform gentamicin in their ability to fight a range of pathogens in vitro. The theories include mechanisms that function against bacteria, including cytoplasmic membrane defects, DNA degradation, bacterial cell wall defects, and interference with bacterial cell division [50, 51]. A study by Bassetti *et al.* [52] found that *Pseudomonas aeruginosa* infections are treated with aminoglycosides like tobramycin, gentamicin, and amikacin. The minimum inhibitory concentration (MIC) is used to evaluate the antimicrobial potency of novel compounds or

Table 1. Measured Optical Density (O.D.) of Biofilm Formation Capability of *Pseudomonas aeruginosa* Isolates.

Isolate <i>pseudomonas aeruginosa</i> No.	O.D.	Isolate <i>Pseudomonas aeruginosa</i> No.	O.D.
<i>Pseudomonas aeruginosa</i> 1	0.253	<i>Pseudomonas aeruginosa</i> 16	0.186
<i>Pseudomonas aeruginosa</i> 2	0.913	<i>Pseudomonas aeruginosa</i> 17	1.23
<i>Pseudomonas aeruginosa</i> 3	0.183	<i>Pseudomonas aeruginosa</i> 18	1.09
<i>Pseudomonas aeruginosa</i> 4	0.860	<i>Pseudomonas aeruginosa</i> 19	0.96
<i>Pseudomonas aeruginosa</i> 5	1.016	<i>Pseudomonas aeruginosa</i> 20	1.08
<i>Pseudomonas aeruginosa</i> 6	0.290	<i>Pseudomonas aeruginosa</i> 21	0.053
<i>Pseudomonas aeruginosa</i> 7	0.276	<i>Pseudomonas aeruginosa</i> 22	0.048
<i>Pseudomonas aeruginosa</i> 8	0.172	<i>Pseudomonas aeruginosa</i> 23	0.153
<i>Pseudomonas aeruginosa</i> 9	0.158	<i>Pseudomonas aeruginosa</i> 24	0.96
<i>Pseudomonas aeruginosa</i> 10	0.073	<i>Pseudomonas aeruginosa</i> 25	1.49
<i>Pseudomonas aeruginosa</i> 11	1.15	<i>Pseudomonas aeruginosa</i> 26	1.92
<i>Pseudomonas aeruginosa</i> 12	1.4	<i>Pseudomonas aeruginosa</i> 27	0.162
<i>Pseudomonas aeruginosa</i> 13	0.280	<i>Pseudomonas aeruginosa</i> 28	1.4
<i>Pseudomonas aeruginosa</i> 14	1.76	<i>Pseudomonas aeruginosa</i> 29	1.06
<i>Pseudomonas aeruginosa</i> 15	0.237	<i>Pseudomonas aeruginosa</i> 30	0.288

Table 2. Minimum inhibitory concentration (MIC) and sub MIC of Gentamicin and Nano-curcumin for *Pseudomonas aeruginosa*.

<i>Pseudomonas aeruginosa</i> isolates	Sub MIC of Gentamicin mg/ml	MIC of Gentamicin mg/ml	Sub MIC of Nano-curcumin mg/ml	MIC of Nano-curcumin mg/ml
<i>Pseudomonas aeruginosa</i> 12	512	1024	128	256
<i>Pseudomonas aeruginosa</i> 14	128	256	64	128
<i>Pseudomonas aeruginosa</i> 25	512	1024	128	256
<i>Pseudomonas aeruginosa</i> 26	256	512	512	1024

**Fig. 11.** The sub minimum inhibitory concentrations (MIC) of Gentamicin and Nano-curcumin against *Pseudomonas aeruginosa*.

extracts by determining how efficiently they reduce antibacterial concentrations. Antibiotics with lower MICs are more effective [53]. Conveyed uses sub-MIC doses of gentamicin and amikacin to decrease the formation of biofilms on plastic components. Several investigations have shown that some pure

compounds, like enzymes and bacteriocins, exhibit strong antibacterial and antibiofilm action and are more effective than gentamicin against a range of infections in vitro. These investigations have also suggested a number of potential antibacterial processes, including disruption of the cytoplasmic

membrane and cell wall, impairment of cell division, and DNA destruction [51]. The minimum inhibitory concentration (MIC) of an antimicrobial agent is the lowest concentration ($\mu\text{g/ml}$) that completely stops the detectable development of a test strain of a bacterium under closely watched laboratory conditions. will be finished. best prediction for the clinical outcome. Antibiotics are used more precisely and effectively [54]. Alternatively, by altering the expression levels of bacterial virulence genes, for example, a minimum inhibitory concentration (sub-MIC) below sub-MIC can influence bacterial pathogenesis [55]. Different phenotypes are caused by gender. According to a study by [56], there are a number of reasons why bacteria are more likely to be encountered through the minimum inhibitory concentration (sub-MIC) of antibiotics, including restricted access to medications and the use of low-dose antibiotics as a preventative measure. The biofilms of earlier isolates were treated with gentamicin and nano-curcumin at minimum inhibitory concentrations (MIC values) [51].

3.7. Antibacterial Activity of Nano-curcumin on *Ps. aeruginosa*

Table 3. shows the antibacterial activity of nano-curcumin against *Ps. aeruginosa* solates at concentrations of 32, 64, 128 and 256 $\mu\text{g/ml}$. The results indicate that nano-curcumin possesses material anti-bacterial activity against all *Ps. aeruginosa* isolates disparity with control, and the anti-bacterial activity of nano-curcumin at 256 $\mu\text{g/ml}$ was significantly higher than 128 $\mu\text{g/ml}$. The sensitivity of *Pseudomonas aeruginosa* to nano-curcumin was measured by a micro-dilution broth assay (Figure 11). Nano-curcumin solutions were

prepared in distilled water and measured by the well diffusion method. The inhibition zone was measured at concentrations of 128 $\mu\text{g/ml}$ and 256 $\mu\text{g/ml}$. Nano-curcumin MICs for four strains of *Pseudomonas aeruginosa* were 128 $\mu\text{g/ml}$ and 256 $\mu\text{g/ml}$ (Figure 12), due to the fact that curcumin nanospheres dissolve more readily [57]. Cur-NPs show strong antibacterial action against *Ps. aeruginosa*, and the outcomes were comparable to those of *Ps. aeruginosa* [58]. Our findings showed that nanoparticles had broad-spectrum inhibitory effects on isolates of *Ps. aeruginosa*. According to an earlier research, curcumin nanoparticles break down bacterial cell walls, and when this happens, the bacteria lyse and die [59]. A mixture of silver nanoparticles and curcumin NPs at 100 $\mu\text{g/ml}$ inhibits 50% of bacterial biofilms, according to another study by Loo *et al.* [60]. Curcumin-coated nanoparticles were found to suppress growth in vitro, according to Krausz *et al.* [61]. Additionally, Alsammarraie *et al.* [62] demonstrated that Ag-Nps

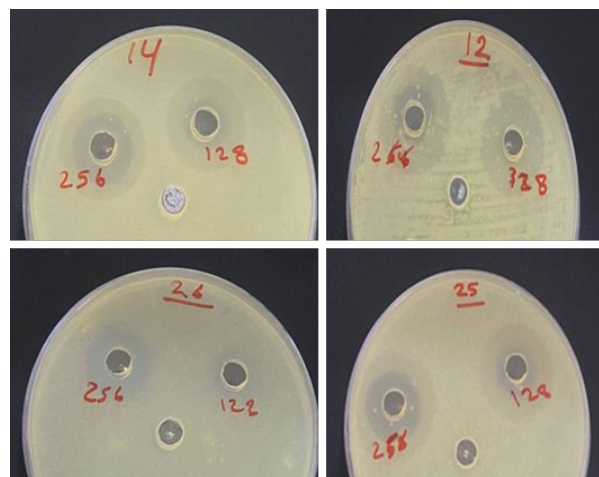


Fig. 12. Antibacterial activity of nano-curcumin against *Pseudomonas aeruginosa* isolates.

Table 3. Antibacterial activity of Curcumin-Ag-Nps on *Pseudomonas aeruginosa* in-vitro.

Treatment	(Mean ± SD) The inhibition zone diameter (mm)				P value
	concentration µg/ml, N = 10				
	32	64	128	256	
Curcumin nano	13.3±5.9a	A 15.3±5.7a	22.3±1.96b	24.3±1b	<0.01 sig
P value	<0.01	<0.01	<0.01	<0.01	

LSD test was used to calculate the significant differences between tested mean, the letters (A, B and C) LSD for rows represented the levels of significant, highly. Similar letters mean there are no significant differences between tested mean. (Sig: significantly).

* Significant differences compared with enzyme and curcumin nano $p < 0.01$.

had antimicrobial properties. Ag-Nps anti-cancer and antioxidant properties have been demonstrated previously [63, 64]. Curcumin's significant action against MRSA and *Staphylococcus aureus* with MLSB resistance phenotype was established in a study by Górski *et al.* [65], with comparable MIC values at a median level of 0.046 mg/ml. Curcumin has been shown to have antibacterial properties against Methicillin-Resistant *Staphylococcus aureus* (MRSA) and *Staphylococcus aureus* [66]. Through its quorum sensing regulation mechanism, curcumin functions as an antibiofilm by inhibiting host receptor attachment, reducing the formation of bacterial biofilms, and other virulence factors [67].

Among all commercially available nanomaterials, Ag-Nps are now the most popular nanoparticles, due to their low toxicity in comparison to other nanoparticles. The initial stage of Ag-Nps nanoparticles' cytotoxic action is usually their adhesion and penetration onto microbial membrane surfaces [15]. Numerous harmful pathogens have been demonstrated to be susceptible to the antibacterial effects of silver [68]. Since ancient times, silver (Ag) has been utilized as a medicinal element; however, modern medical research is examining the properties and uses of silver nanoparticles (Ag-Nps). Silver is used in modern antibacterial salve and unguents to prevent microbiological spread of burns and open wounds. Additionally, silver is frequently utilized in implants and medical equipment composed of polymers doped with silver, a lot of silver-based consumer goods, like colloidal silver gels and fabrics with silver embedded in them, are currently utilized in athletic wear [69]. Together with various polysaccharides and essential oils, these substances greatly enhance the plant's antimicrobial qualities.

In this investigation, all isolates formed biofilms, with 53.3% exhibiting strong biofilm formation, 36.7% exhibiting moderate biofilm formation, and 10% exhibiting weak biofilm development. This study's findings were consistent with those of Freeman *et al.* [31], which is one of the primary factors that slows the healing process of burn infections. In burn infections, *Ps. aeruginosa* forms biofilms at a high rate. The optical density was found to differ significantly before and after treatment with nano-curcumin. This study examines the antibacterial and anti-biofilm properties of nanocurcumin against strains

of *Pseudomonas aeruginosa*, one of the major infections in Iraq.

4. CONCLUSIONS

Biosynthesis of curcumin-Ag is a clean, inexpensive, and safe method, where no toxic substances were used, and thus it has no side effects. Since many pathogenic microbes have gained resistance to antibiotics, the combination of curcumin with several nanoparticles will be helpful in treating pathogenic. The anti-bacterial activity of nano-curcumin at 256 µg/ml was significantly higher against all MDR *Ps. aeruginosa* isolates disparity with control. The phytochemical composition of turmeric, and the content of its primary biologically active compounds, most notably curcumin contribute significantly to the antimicrobial properties.

5. ACKNOWLEDGMENTS

The authors would like to thank Mustansiriyah University (www.uomustansiriyah.edu.iq) and Department Microbiology, Faculty Veterinary medicine, Urmia University for providing the necessary laboratories and necessary spectral facilities.

6. ETHICAL APPROVAL

This study does not involve experiments on animals or human subjects.

7. CONFLICT OF INTEREST

The authors report no financial or any other conflicts of interest in this work.

8. REFERENCES

1. G.H.R.V. de Macedo, G.D.E. Costa, E.R. Oliveira, G.V. Damasceno, J.S.P. Mendonça, L.S. Silva, V.L. Chagas, J.M.N. Bazán, A.S.D.S. Aliança, R.C.M. Miranda, A. Zigmignan, A.S. Monteiro, and L.C.N. Silva. Interplay between ESKAPE Pathogens and Immunity in Skin Infections: An Overview of the Major Determinants of Virulence and Antibiotic Resistance. *Pathogens* 10(2): 148 (2021).
2. M.Y. Memar, K. Adibkia, S. Farajnia, S.M. Kafil, Y. Khalili, R. Azargun, and R. Ghotaslou. *In-vitro* effect of imipenem, fosfomycin, colistin, and gentamicin combination against carbapenem-

- resistant and biofilm-forming *Pseudomonas aeruginosa* isolated from burn patients. *Iranian Journal of Pharmaceutical Research* 20(2): 286 (2021).
3. M. Gholami, H. Zeighami, R. Bikas, A. Heidari, F. Rafiee, and F. Haghi. Inhibitory activity of metal-curcumin complexes on quorum sensing related virulence factors of *Pseudomonas aeruginosa* PAO1. *AMB Express* 10(1): 111 (2020).
 4. L.H. Mahdi, A.B. Hasson, M.G. Sulaiman, A.H. Mohammed, H.K. Jawad, G.A. Al- Dulmi, H.R. Essa, S. Albukhaty, and R. Khan. Anti-microbial efficacy of L-glutaminase (EC 3.5.1.2) against multidrug-resistant *Pseudomonas aeruginosa* infection. *Journal Antibiotics* 77(2): 111-119 (2024).
 5. A. Kunwar, P.P. Shrestha, S. Shrestha, S. Thapa, S. Shrestha, and N.M. Amatya. Detection of biofilm formation among *Pseudomonas aeruginosa* isolated from burn patients. *Burns Open* 5: 125–129 (2021).
 6. R.K. Raghavendhar and L.L. Devanand. Curcumin: Biological, Pharmaceutical, Nutraceutical, and Analytical Aspects. *Molecules* 24(16): 2930 (2019).
 7. S.G. Gupta, S. Patchva, and B.B. Aggarwal. Therapeutic roles of curcumin: lessons learned from clinical trials. *AAPS Journal* 15(1): 195-218 (2013).
 8. A. Gupta, S.M. Briffa, S.Swingle, H.Gibson, V. Kannappan, G. Adamus, M. Kowalczyk, C. Martin, and I. Radecka. Synthesis of Silver Nanoparticles Using Curcumin-Cyclodextrins Loaded into Bacterial Cellulose-Based Hydrogels for Wound Dressing Applications. *Biomacromolecules* 21(5): 1802-1811 (2020).
 9. A. Gupta, D.J. Keddie, V. Kannappan, H.Gibson, I.R. Khalil, M. Kowalczyk, C. Martin, X. Shuai, and I. Radecka. Production and characterisation of bacterial cellulose hydrogels loaded with curcumin encapsulated in cyclodextrins as wound dressings. *European Polymer Journal* 118: 437-450 (2019).
 10. Z. Song, Y. Wu, H. Wang, and H. Han. Synergistic antibacterial effects of curcumin modified silver nanoparticles through ROS-mediated pathways. *Materials Science & Engineering: C* 99: 255-263 (2019).
 11. M. Fahim, A. Shahzaib, N. Nishat, A. Jahan, T.A. Bhat, and A. Inam. Green synthesis of silver nanoparticles: A comprehensive review of methods, influencing factors, and applications. *JCIS Open* 16: 100125 (2024).
 12. Y. Lyu, M. Yu, Q. Liu, Q. Zhang, Z. Liu, Y. Tian, D. Li, and M. Changdao. Synthesis of silver nanoparticles using oxidized amylose and combination with curcumin for enhanced antibacterial activity. *Carbohydrate Polymers* 230: 115573 (2020).
 13. E. Vetchinkina, E. Loshchinina, M. Kupryashina, A. Burov, T. Pylaev. and V. Nikitina. Green synthesis of nanoparticles with extracellular and intracellular extracts of basidiomycetes. *Peer J* 6: e5237 (2018).
 14. H. Matthew, D. Melissa, D. Maria, and G. Anisha Gup. Green Synthesis of Nanomaterials. *Nanomaterials* 11(8): 2130 (2021).
 15. S. Khorrami, A. Zarrabi, M. Khaleghi, M. Danaei, and M.R. Mozafari. Selective cytotoxicity of green synthesized silver nanoparticles against the MCF-7 tumor cell line and their enhanced antioxidant and antimicrobial properties. *International Journal of Nanomedicine* 13: 8013-8024 (2018).
 16. D. Hatice, E. Furkan, A.S. Emir, M.W. Anna, B.I. Mikhael, and K. Sercan. Silver Nanoparticles: A Comprehensive Review of Synthesis Methods and Chemical and Physical Properties. *Nanomaterials* 14(18): 1527 (2024).
 17. I. Hussain, N.B. Singh, A. Singh, H. Singh, and S.C. Singh. Green synthesis of nanoparticles and its potential application. *Biotechnology Letters* 38: 545-560 (2016).
 18. M.J. Khan, K. Shameli, A.Q. Sazili, J. Selamat, and S.Kumari. Rapid Green Synthesis and Characterization of Silver Nanoparticles Arbitrated by Curcumin in an Alkaline Medium. *Molecules* 24(4): 719 (2019).
 19. V. Gopinath, D.M. Ali, S. Priyadarshini, N.M. Priyadharsshini, N. Thajuddin, and P.Velusamy. Biosynthesis of silver nanoparticles from *Tribulus terrestris* and its antimicrobial activity: A novel biological approach. *Colloids and Surfaces B: Biointerfaces* 96: 69-74 (2012).
 20. S. Basavaraja, S.D. Balaji, A. Lagashetty, A.H. Rajasab, and A. Venkataraman. Extracellular biosynthesis of silver nanoparticles using the fungus *Fusarium semitectum*. *Materials Research Bulletin* 43(5): 1164-1170 (2008).
 21. C.C. González, L.I.G. García, L.G.B. Jurado, and A.C. Castillo. Bactericidal activity of silver nanoparticles in drug-resistant bacteria. *Brazilian Journal of Microbiology* 54: 691-701 (2023).
 22. A. Rai, S. Seena, T. Gagliardi, and P.J. Palma. Advances in the design of amino acid and peptide synthesized gold nanoparticles for their applications. *Advances in Colloid and Interface Science* 318: 102951 (2023).
 23. A.K. Keshari, R. Srivastava, P. Singh, V.B. Yadav, and G. Nath. Antioxidant and antibacterial activity of silver nanoparticles synthesized by *Cestrum nocturnum*. *Journal of Ayurveda and Integrative*

- Medicine* 11(1): 37-44 (2020).
24. S. Browne, S. Bhatia, N. Sarkar, and M. Kaushik. Antibiotic-resistant bacteria and antibiotic-resistant genes in agriculture: a rising alarm for future. In: Degradation of Antibiotics and Antibiotic-Resistant Bacteria from Various Sources. P. Singh and M. Sillanpää (Eds.). *Academic Press* pp. 247-274 (2023).
 25. E.S. Nazoori and A. Kariminik. In Vitro Evaluation of Antibacterial Properties of Zinc Oxide Nanoparticles on Pathogenic Prokaryotes. *Journal of Applied Biotechnology Reports* 5(4): 162-165 (2018).
 26. G. Stati, F. Rossi, T. Trakoolwilaiwan, D.L. Tung, S. Mourdikoudis, N.T.K. Thanh, and R.D. Pietro. Development and Characterization of Curcumin-Silver Nanoparticles as a Promising Formulation to Test on Human Pterygium-Derived Keratinocytes. *Molecules* 27(1): 282 (2022).
 27. S. Bettini, R. Pagano, L. Valli, and G. Giancane. Drastic nickel ion removal from aqueous solution by curcumin-capped Ag nanoparticles. *Nanoscale* 6: 10113-10117 (2014).
 28. A. Shariati, E. Asadian, F. Fallah, T. Azimi, A. Hashemi, J.Y. Sharahi, and M.T. Moghadam. Evaluation of Nano-curcumin effects on expression levels of virulence genes and biofilm production of multidrug-resistant *Pseudomonas aeruginosa* isolated from burn wound infection in Tehran, Iran. *Infection and Drug Resistance* 12: 2223-2235 (2019).
 29. Clinical and Laboratory Standards Institute (CLSI). Performance standards for antimicrobial susceptibility testing. *Clinical and Laboratory Standards Institute, Wayne PA, USA* (2020). <https://www.nih.org.pk/wp-content/uploads/2021/02/CLSI-2020.pdf>.
 30. A.P. Magiorakos, A. Srinivasan, R.B. Carey, Y. Carmeli, M.E. Falagas, C.G. Giske, S. Harbarth, J.F. Hindler, G. Kahlmeter, B.O. Liljequist, D.L. Paterson, L.B. Rice, J. Stelling, M.J. Struelens, A. Vatopoulos, J.T. Weber, and D.L. Monnet. Multidrug-resistant, extensively drug-resistant and pandrug-resistant bacteria: an international expert proposal for interim standard definitions for acquired resistance. *Clinical Microbiology and Infection* 18(3): 268-281 (2012).
 31. D.J. Freeman, F.R. Falkner, and K.C.T. Keane. New method for detecting slime production by Coagulase negative staphylococci. *Journal of Clinical Pathology* 42(8): 872-874 (1989).
 32. R.M.S. AL-Oqaili. Use Ethidium Bromide as curing to plasmid in *Staphylococcus aureus* (MRSA) isolated from Patients Iraqi and Screening for Virulence Factors. *Journal of Pharmaceutical Sciences and Research* 10(9): 2351-2353 (2018).
 33. D. Zhang, J. Xia, Y. Xu, M. Gong, Y. Zhou, L. Xie, and X. Fang. Biological features of biofilm-forming ability of *Acinetobacter baumannii* strains derived from 121 elderly patients with hospital-acquired pneumonia. *Clinical and Experimental Medicine* 16: 73-80 (2016).
 34. S. Sandhuli, P. Shashiprabha, A.N. Dunuweera, N. Dunuweera, and R.M.G. Rajapakse. Synthesis of Curcumin Nanoparticles from Raw Turmeric Rhizomes. *ACS Omega* 6(12): 8246-8252 (2021).
 35. M. Elshikh, S. Ahmed, S. Funston, P. Dunlop, M. McGaw, R. Marchant, and I.M. Banat. Resazurin-based 96-well plate microdilution method for the determination of minimum inhibitory concentration of biosurfactants. *Biotechnology Letters* 38: 1015-1019 (2016).
 36. S. Stepanovic, D. Vukovic, V. Hola, G.D. Bonaventura, S. Djukic, I. Cirkovic, and F. Ruzicka. Quantification of biofilm in microtiter plates: overview of testing conditions and practical recommendations for assessment of biofilm production by Staphylococci. *Acta Pathologica, Microbiologica et Immunologica Scandinavica (APMIS)* 115(8): 891-899 (2007).
 37. A. Kunwar, P. Shrestha, S. Shrestha, S. Thapa, S. Shrestha, and N.M. Amatya. Detection of biofilm formation among *Pseudomonas aeruginosa* isolated from burn patients. *Burns Open* 5(3): 125-129 (2021).
 38. R. Aakash, Kavyarathna, G.S. Nagananda, T.R. Kavya, R. Reddy, K.U. Minchitha, S. Swetha, and S. Suryan. Synergistic blend: Curcumin-loaded silver nanoparticles synthesized from *Talaromyces atrovirens* pigment for bio evaluation. *Plant Nano Biology* 10: 100120 (2024).
 39. I. Ali, M. Ali, A.B. Ahmed, and H.I. Al-Ahmed. Green synthesis and characterization of silver nanoparticles for reducing the damage to sperm parameters in diabetic compared to metformin. *Scientific Reports* 13: 2256 (2023).
 40. M.M. Gevorgyan, N.P. Voronina, N.V. Goncharova, T.V. Kozaruk, G.S. Russkikh, L.A. Bogdanova, and T.A. Korolenko. Cystatin C as a Marker of Progressing Cardiovascular Events during Coronary Heart Disease. *Bulletin of Experimental Biology and Medicine* 162(10): 421-424 (2017).
 41. A. Joly and M.S. Latha. Synthesis of Nano-curcumin-Alginate Conjugate and its Characterization by

- XRD, IR, UV-VIS Andaman Spectroscopy. *Oriental Journal of Chemistry* 35(2): 751 (2019).
42. M.P. Gashti, F. Alimohammadi, A. Kiumarsi, W. Nogala, Z. Xu, W.J. Eldridge, and A. Wax. In: *Nanocomposite Materials: Synthesis, Properties and Applications*. J. Parameswaranpillai, N. Hameed, T. Kurian, and Y. Yu (Eds.). 1st Edition. Chapter 5. *CRC Press, Taylor & Francis, Boca Raton* (2016).
 43. V.A. Hackley and J.D. Clogston. Measuring the Hydrodynamic Size of Nanoparticles in Aqueous Media Using Batch-Mode Dynamic Light Scattering. In: *Methods in Molecular Biology: Characterization of Nanoparticles Intended for Drug Delivery*. S.E. McNeil (Editor). Volume 697. *Humana Press* pp. 35-52 (2011).
 44. T. Zheng, S. Bott, and Q. Huo. Techniques for Accurate Sizing of Gold Nanoparticles Using Dynamic Light Scattering with Particular Application to Chemical and Biological Sensing Based on Aggregate Formation. *ACS Applied Materials & Interfaces* 8(33): 21585-21594 (2016).
 45. J. Lim, S.P. Yeap, H.X. Che, and S.C. Low. Characterization of magnetic nanoparticle by dynamic light scattering. *Nanoscale Research Letters* 8(1): 381 (2013).
 46. F. Kesisoglou, S. Panmai, and Y. Wu. Nanosizing-oral formulation development and biopharmaceutical evaluation. *Advanced Drug Delivery Reviews* 59(7): 631-644 (2007).
 47. S. Mohanty, B. Baliyarsingh, and S.K. Nayak. Antimicrobial Resistance in *Pseudomonas aeruginosa*: A Concise Review. In: *Antimicrobial Resistance - A One Health Perspective*. M. Mareş, S.H.E. Lim, K.S. Lai, and R.T. Cristina (Eds.). Chapter 3. *Intech Open* (2020).
 48. O.A. Akingbade, S.A. Balogun, D.A. Ojo, R.O. Afolabi, B.O. Motayo, P.O. Okerentugba, and I.O. Okonko. Plasmid profile analysis of multidrug resistant *Pseudomonas aeruginosa* isolated from wound Infections in Southwest, Nigeria. *World Applied Sciences Journal* 20(6): 766-775 (2012).
 49. A. Litwin, O. Fedorowicz, and W. Duszynska. Characteristics of Microbial Factors of Healthcare-Associated Infections Including Multidrug-Resistant Pathogens and Antibiotic Consumption at the University Intensive Care Unit in Poland in the Years 2011-2018. *International Journal of Environmental Research and Public Health* 17(19): 6943 (2020).
 50. L.H. Mahdi, N.Z. Mahdi, R.M. Sajet, I.G. Auda, H.N. Mater, L.A. Zwain, and L.G. Alsaadi. Anticariogenic and antibiofilm of purified bacteriocin of *Lactobacillus curvatus* and immunomodulatory effect of *L. curvatus* in streptococcal bacteremia. *Reviews and Research in Medical Microbiology* 30(1): 26-35 (2019).
 51. L.M. Mahdi, A.R. Laftah, K.H. Yaseen, I.G. Auda, and R.H. Essa. Establishing novel roles of bifidocin LHA, antibacterial, antibiofilm and immunomodulator against *Pseudomonas aeruginosa* corneal infection model. *International Journal of Biological Macromolecules* 186: 433-444 (2021).
 52. M. Bassetti, A. Vena, E. Righi, A. Croxatto, and B. Guery. How to manage *Pseudomonas aeruginosa* infections. *Drugs in Context* 7: 212527 (2018).
 53. D. Nigussie, G. Davey, B.A. Legesse, A. Fekadu, and E. Makonnen. Antibacterial activity of methanol extracts of the leaves of three medicinal plants against selected bacteria isolated from wounds of lymphoedema patients. *BMC Complementary Medicine and Therapies* 21: 2 (2021).
 54. K.B. Kowalska and W.R. Dudek. The minimum inhibitory concentration of antibiotics: methods, interpretation, clinical relevance. *Pathogens* 10(2): 165 (2021).
 55. G.F. Sanz, A.S. Hernando, and J.L. Martínez. Evolution under low antibiotic concentrations: A risk for the selection of *Pseudomonas aeruginosa* multidrug-resistant mutants in nature. *Environmental Microbiology* 24(3): 1279-1293 (2022).
 56. N. Saidi, F. Davarzani, Z. Yousefpour, and P. Owlia. Effects of Sub-Minimum Inhibitory Concentrations of Gentamicin on Alginate Produced by Clinical Isolates of *Pseudomonas aeruginosa*. *Advanced Biomedical Research* 12(1): 94 (2023).
 57. W.H. Lee, C.Y. Loo, M. Bebawy, F. Luk, R. Mason, and R. Rohanizadeh. Curcumin and its Derivatives: Their Application in Neuropharmacology and Neuroscience in the 21st Century. *Current Neuropharmacology* 11(4): 338-378 (2013).
 58. N. El-Kattan, A.N. Emam, A.S. Mansour, M.A. Ibrahim, A.B.A. El-Razik, K.A.M. Allam, N.M. Riadi, and S.A. Ibrahim. Curcumin assisted green synthesis of silver and zinc oxide nanostructures and their antibacterial activity against some clinical pathogenic multi-drug resistant bacteria. *RSC Advances* 12: 18022-18038 (2022).
 59. S. Roudashti, H. Zeighami, H. Mirshahabi, S. Bahari, A. Soltani, and F. Haghi. Synergistic activity of sub-inhibitory concentrations of curcumin with ceftazidime and ciprofloxacin against *Pseudomonas aeruginosa* quorum sensing related genes and virulence traits. *World Journal of Microbiology and*

- Biotechnology* 33: 50 (2017).
60. C.Y. Loo, R. Rohanizadeh, P.M. Young, D. Traini, R. Cavaliere, C.B. Whitchurch, and W.H. Lee. Combination of silver nanoparticles and curcumin nanoparticles for enhanced anti-biofilm activities. *Journal of Agricultural and Food Chemistry* 64(12): 2513-2522 (2016).
 61. A.E. Krausz, B.L. Adler, V. Cabral, M. Navati, J. Doerner, R.A. Charafeddine, D. Chandra, H. Liang, L. Gunther, A. Clendaniel, S. Harper, J.M. Friedman, J.D. Nosanchuk, and A.J. Friedman. Curcumin-encapsulated nanoparticles as innovative antimicrobial and wound healing agent. *Nanomedicine: Nanotechnology, Biology and Medicine* 11(1): 195-206 (2015).
 62. F.K. Alsammarräie, W. Wang, P. Zhou, A. Mustapha, and M. Lin. Green Synthesis of Silver Nanoparticles Using Turmeric Extracts and Investigation of Their Antibacterial Activities. *Colloids Surfaces B: Biointerfaces* 171: 398-405 (2018).
 63. A.D. Selvan, D. Mahendiran, K.R. Senthil, and K.A. Rahiman. Garlic, Green tea and Turmeric Extracts-Mediated Green Synthesis of Silver Nanoparticles: Phytochemical, Antioxidant and in Vitro Cytotoxicity Studies. *Journal of Photochemistry and Photobiology B: Biology* 180: 243-252 (2018).
 64. X.X. Yang, C.M. Li, and C.Z. Huang. Curcumin Modified Silver Nanoparticles for Highly Efficient Inhibition of Respiratory Syncytial Virus Infection Xiao. *Nanoscales* 8(5): 3040-3048 (2016).
 65. M. Górski, J. Niedźwiadek, and A. Magryś. Antibacterial activity of curcumin – a natural phenylpropanoid dimer from the rhizomes of *Curcuma longa* L. and its synergy with antibiotics. *Annals of Agricultural and Environmental Medicine* 29(3): 394-400 (2022).
 66. A.M. El-Mahdy, M. Alqahtani, M. Almukainzi, M.F. Alghoribi, and S.H.A. Abdel-Rhman. Effect of Resveratrol and Curcumin on Gene Expression of Methicillin-Resistant *Staphylococcus aureus* (MRSA) Toxins. *Journal of Microbiology and Biotechnology* 34(1): 141-148 (2024).
 67. D. Zheng, C. Huang, H. Huang, Y. Zhao, M.R.U. Khan, H. Zhao, and L. Huang. Antibacterial mechanism of curcumin: A review. *Chemistry & Biodiversity* 17(8): e2000171 (2020).
 68. M. Oves, M. Aslam, M.A. Rauf, S. Qayyum, H.A. Qari, M.S. Khan, M.Z. Alam, S. Tabrez, A. Pugazhendhi, and I.M.I. Ismail. Antimicrobial and anticancer activities of silver nanoparticles synthesized from the root hair extract of *Phoenix dactylifera*. *Materials Science & Engineering C: Materials for Biological Applications* 89: 429-443 (2018).
 69. R. Shanmuganathan, I. Karuppusamy, M. Saravanan, H. Muthukumar, K. Ponnuchamy, V.S. Ramkumar, and A. Pugazhendhi. Synthesis of Silver Nanoparticles and their Biomedical Applications - A Comprehensive Review. *Current Pharmaceutical Design* 25(24): 2650-2660 (2019).